



**INTERNATIONAL JOURNAL OF  
PHARMACEUTICAL SCIENCES**  
[ISSN: 0975-4725; CODEN(USA): IJPS00]  
Journal Homepage: <https://www.ijpsjournal.com>



## Research Paper

# Development and Evaluation of Essential Oil-Enriched Topical Hydrogels for Antimicrobial Activity Against Anaerobic Pathogens Associated with Gas Gangrene

Hritik\*, Dr. Puneet Kumar, Naresh Kumar

*Dreamz College of pharmacy Khilra, Sundernagr.*

### ARTICLE INFO

Published: 07 July 2026

**Keywords:**

Essential oils; Hydrogel;  
Gas gangrene; Clostridium  
perfringens; Biofilm;  
Antimicrobial activity;  
Topical drug delivery.

**DOI:**

10.5281/zenodo.21242405

### ABSTRACT

Gas gangrene is a rapidly progressing necrotizing infection caused primarily by anaerobic pathogens such as Clostridium perfringens and Clostridium septicum. The present study aimed to develop and optimize a topical hydrogel formulation enriched with a synergistic blend of eucalyptus, clove, and neem essential oils for enhanced antimicrobial activity against anaerobic pathogens. Hydrogel formulations were prepared using carbomer and hydroxypropyl methylcellulose (HPMC) as polymeric bases and optimized using a Box–Behnken design. The formulations were evaluated for physicochemical properties, in vitro drug release, antimicrobial activity, antibiofilm efficacy, ex vivo permeation, cytocompatibility, and stability. The optimized formulation (F13) exhibited acceptable pH ( $5.61 \pm 0.01$ ), viscosity ( $5200 \pm 150$  cP), spreadability ( $18.0 \pm 0.5$  g·cm/s), and drug content ( $98.9 \pm 1.0\%$ ). Sustained drug release was observed over 12 hours, with Korsmeyer–Peppas kinetics indicating non-Fickian diffusion behavior. The optimized formulation demonstrated significant antimicrobial activity with a minimum inhibitory concentration of 18 µg/mL and showed strong bactericidal activity in time–kill studies. Biofilm inhibition and eradication studies revealed  $85.6 \pm 2.7\%$  and  $80.2 \pm 2.6\%$  activity, respectively. Ex vivo permeation studies showed enhanced permeation with a flux of  $78.4 \pm 2.4$  µg/cm<sup>2</sup>/hr. Cytocompatibility studies demonstrated acceptable cell viability ( $86.4 \pm 1.9\%$ ). Stability studies confirmed minimal changes in physicochemical parameters over three months. The findings suggest that the developed essential oil-enriched hydrogel possesses significant potential for topical management of anaerobic wound infections associated with gas gangrene.

\*Corresponding Author: Hritik

Address: *Dreamz College of pharmacy Khilra, Sundernagr.*

Email ✉: [hritikmandyal1016@gmail.com](mailto:hritikmandyal1016@gmail.com)

**Relevant conflicts of interest/financial disclosures:** The authors declare that the research was conducted in the absence of any commercial or financial relationships that could be construed as a potential conflict of interest.



## INTRODUCTION

Gas gangrene is a severe and rapidly progressing necrotizing infection characterized by extensive tissue destruction, gas production, and systemic toxicity. The disease is primarily associated with anaerobic bacterial pathogens such as *Clostridium perfringens* and *Clostridium septicum*, which produce potent exotoxins capable of causing rapid myonecrosis and vascular damage. The condition frequently develops in traumatic wounds, ischemic tissues, or post-surgical infections where oxygen tension is significantly reduced, creating a favourable environment for clostridial proliferation (Ghanouni *et al.*, 2022; Huang *et al.*, 2022; Jia *et al.*, 2025; Wu *et al.*, 2025).

Despite advances in antimicrobial therapy and surgical management, gas gangrene remains associated with considerable morbidity and mortality. Conventional treatment strategies primarily involve aggressive surgical debridement combined with systemic antibiotic therapy. However, several limitations are associated with these approaches. Antibiotic penetration into necrotic tissue is often inadequate due to impaired vascularization, while the anaerobic environment reduces the effectiveness of many antimicrobial agents. Furthermore, the emergence of antimicrobial resistance and biofilm-associated infections has complicated the management of anaerobic wound infections (Huang *et al.*, 2022; Jia *et al.*, 2025; Woog & Destro, 2022; Wu *et al.*, 2025).

Biofilm formation represents a major challenge in chronic and necrotizing infections. Biofilms are structured microbial communities enclosed within a self-produced extracellular polymeric matrix that protects bacteria from antibiotics and host immune responses. This protective mechanism contributes to persistent infections, delayed healing, and increased resistance to treatment. Therefore, there is an urgent need for alternative therapeutic

systems capable of targeting anaerobic pathogens and disrupting biofilm structures (Huang *et al.*, 2022; Jia *et al.*, 2025; Su *et al.*, 2026; Woog & Destro, 2022; Wu *et al.*, 2025).

In recent years, plant-derived essential oils have gained considerable attention as potential antimicrobial agents due to their broad-spectrum activity and multi-target mechanisms of action. Essential oils contain complex mixtures of terpenoids, phenolics, and aromatic compounds capable of disrupting microbial cell membranes, interfering with metabolic processes, and inducing oxidative stress. Among various essential oils, eucalyptus oil, clove oil, and neem oil have demonstrated promising antimicrobial and wound-healing properties.

Eucalyptus oil, rich in 1,8-cineole, possesses strong antimicrobial and penetration-enhancing properties. Clove oil contains eugenol, a phenolic compound known for potent bactericidal and anti-inflammatory activity. Neem oil exhibits antimicrobial, antioxidant, and wound-healing effects due to the presence of bioactive compounds such as azadirachtin and nimbidin. The synergistic combination of these oils may enhance antimicrobial efficacy while reducing the required concentration of individual components (Qi *et al.*, 2026; Sha *et al.*, 2026; Sharma *et al.*, 2026; Shi *et al.*, 2026; Trinh *et al.*, 2026; Vater *et al.*, 2026; Vaz *et al.*, 2026; Wang *et al.*, 2026).

However, the practical application of essential oils is limited by their poor aqueous solubility, volatility, and instability. To overcome these limitations, incorporation into suitable drug delivery systems is necessary. Hydrogels have emerged as effective topical delivery platforms due to their high water content, biocompatibility, controlled release behaviour, and ability to maintain a moist wound environment. The incorporation of essential oils into hydrogel matrices can enhance stability, improve retention at the application site, and facilitate sustained drug



release (Farruggia *et al.*, 2024; Fernandes *et al.*, 2024; Filipe *et al.*, 2022; Fincheira *et al.*, 2024). Therefore, the present study aimed to develop and optimize a topical hydrogel formulation enriched with a synergistic blend of eucalyptus, clove, and neem essential oils for enhanced antimicrobial activity against anaerobic pathogens associated with gas gangrene.

## 2. MATERIALS AND METHODS

### 2.1 Materials

Eucalyptus oil (*Eucalyptus globulus*), clove oil (*Syzygium aromaticum*), and neem oil (*Azadirachta indica*) were procured from certified pharmaceutical suppliers and used as active antimicrobial agents in the formulation development process. Carbomer 934 and hydroxypropyl methylcellulose (HPMC) were used as polymeric gelling agents for hydrogel preparation. Tween 80 served as the surfactant for essential oil dispersion, while propylene glycol was used as a cosolvent and penetration enhancer. Triethanolamine was used for pH adjustment and gel neutralization. All solvents and reagents employed in the study were of analytical grade.

### 2.2 Preformulation Studies

#### 2.2.1 Organoleptic Evaluation of Essential Oils

The procured essential oils were subjected to organoleptic evaluation to determine their appearance, colour, Odor, and clarity under normal daylight conditions (Adena *et al.*, 2021; Ismail *et al.*, 2021; Jain *et al.*, 2021; Raj *et al.*, 2026; Weimer *et al.*, 2026).

#### 2.2.2 Gas Chromatography–Mass Spectrometry (GC–MS) Analysis

GC–MS analysis was carried out to identify major phytochemical constituents present in the essential oils. The analysis was performed using a GC–MS system equipped with a capillary column under

optimized chromatographic conditions. The obtained spectra were compared with standard spectral libraries for compound identification (Adena *et al.*, 2021; Ismail *et al.*, 2021; Jain *et al.*, 2021; Raj *et al.*, 2026; Weimer *et al.*, 2026).

#### 2.2.3 Fourier Transform Infrared (FT-IR) Compatibility Study

Compatibility studies between essential oils and selected excipients were performed using FT-IR spectroscopy. Samples were mixed with potassium bromide and compressed into pellets before analysis over a scanning range of 4000–400  $\text{cm}^{-1}$  (Adena *et al.*, 2021; Ismail *et al.*, 2021; Jain *et al.*, 2021; Raj *et al.*, 2026; Weimer *et al.*, 2026).

### 2.3 Experimental Design

A three-factor, three-level Box–Behnken design was employed for optimization of the hydrogel formulations. The independent variables included essential oil concentration, surfactant concentration, and polymer concentration. The dependent variables selected for optimization included viscosity, spreadability, drug release, and antimicrobial activity. Design-Expert® software was used for statistical optimization and analysis of experimental responses (Adena *et al.*, 2021; Ismail *et al.*, 2021; Jain *et al.*, 2021; Raj *et al.*, 2026; Weimer *et al.*, 2026).

### 2.4 Preparation of Essential Oil-Enriched Hydrogels

Hydrogel formulations were prepared using carbomer 934 and hydroxypropyl methylcellulose (HPMC) as polymeric bases. Carbomer was dispersed in purified water and allowed to hydrate overnight. HPMC solution was prepared separately under continuous stirring. The essential oil blend containing eucalyptus oil, clove oil, and neem oil was prepared in a fixed ratio and mixed with Tween 80 and propylene glycol to obtain a homogeneous oil phase. The oil phase was gradually incorporated into the hydrated



polymeric dispersion with continuous stirring. Triethanolamine was added dropwise until a uniform gel consistency was obtained. The final weight of each formulation was adjusted with purified water (Koillpillai & Narayanasamy, 2024; Singh *et al.*, 2026; Tang *et al.*, 2024; Vemula *et al.*, 2024).

## 2.5 Evaluation of Hydrogel Formulations

### 2.5.1 Determination of pH

The pH of the prepared hydrogel formulations was measured using a calibrated digital pH meter at room temperature (Alves *et al.*, 2022; Beraldo-Araújo *et al.*, 2022; Haimhoffer *et al.*, 2021; Santonocito *et al.*, 2022; Steele & Austin, 2016).

### 2.5.2 Viscosity Measurement

Viscosity measurements were carried out using a Brookfield viscometer fitted with appropriate spindle assembly at controlled rotational speed.

### 2.5.3 Spreadability Study

Spreadability of the formulations was determined using the glass slide method. The time required for separation of slides under applied weight was recorded and used for calculation (Ameur *et al.*, 2022; Azevedo *et al.*, 2022; Azizpour *et al.*, 2025; Baccouri *et al.*, 2008).

### 2.5.4 Drug Content Determination

Drug content uniformity was evaluated by dissolving a known quantity of hydrogel in ethanol followed by spectrophotometric analysis of extracted active components (Ameur *et al.*, 2022; Azevedo *et al.*, 2022; Azizpour *et al.*, 2025; Baccouri *et al.*, 2008).

## 2.6 In Vitro Drug Release Study

In vitro drug release studies were carried out using Franz diffusion cells fitted with dialysis membranes. The receptor compartment was filled with phosphate buffer (pH 6.8) maintained at  $37 \pm$

$0.5^\circ\text{C}$  under continuous stirring conditions. Aliquots were withdrawn at predetermined time intervals and replaced with fresh receptor medium. Samples were analyzed spectrophotometrically to determine cumulative drug release (Ameur *et al.*, 2022; Azevedo *et al.*, 2022; Azizpour *et al.*, 2025; Baccouri *et al.*, 2008).

## 2.7 Drug Release Kinetics

The release data obtained from in vitro drug release studies were fitted into various kinetic models, including (Ameur *et al.*, 2022; Azevedo *et al.*, 2022; Azizpour *et al.*, 2025; Baccouri *et al.*, 2008):

- Zero-order model
- First-order model
- Higuchi diffusion model
- Korsmeyer–Peppas model

Correlation coefficients ( $R^2$  values) were used to determine the best-fit model and release mechanism.

## 2.8 Antimicrobial Activity

### 2.8.1 Minimum Inhibitory Concentration (MIC) and Minimum Bactericidal Concentration (MBC)

Antimicrobial activity was evaluated against anaerobic pathogens associated with gas gangrene, including *Clostridium perfringens* and *Clostridium septicum*. MIC and MBC values were determined using broth microdilution techniques under anaerobic incubation conditions (Ahmed Khan & van Vuuren, 2021; Wu *et al.*, 2025; Xu *et al.*, 2026; Yang *et al.*, 2026; Zhang *et al.*, 2026).

### 2.8.2 Time–Kill Kinetics Study

Time–kill studies were performed by exposing bacterial suspensions to optimized hydrogel formulations at concentrations equivalent to  $1 \times$  MIC and  $2 \times$  MIC. Viable bacterial counts were determined at predetermined intervals (Xu *et al.*, 2026; Yang *et al.*, 2026; Zhang *et al.*, 2026).



### 2.8.3 Checkerboard Assay and Synergy Analysis

Synergistic interaction among essential oils was evaluated using the checkerboard assay. Fractional inhibitory concentration index (FICI) values were calculated to determine the nature of interaction (Xu *et al.*, 2026; Yang *et al.*, 2026; Zhang *et al.*, 2026).

### 2.9 Antibiofilm Activity

Biofilm inhibition and eradication studies were performed using crystal violet staining methods. The ability of hydrogel formulations to inhibit biofilm formation and disrupt preformed biofilms was evaluated spectrophotometrically (Xu *et al.*, 2026; Yang *et al.*, 2026; Zhang *et al.*, 2026).

### 2.10 Ex Vivo Permeation Study

Ex vivo permeation studies were carried out using Franz diffusion cells fitted with excised biological membranes. The receptor compartment contained phosphate buffer maintained at controlled temperature and stirring conditions. Samples were collected at predetermined intervals and analyzed to determine cumulative permeation and flux values.

### 2.11 Cytocompatibility Study

The cytocompatibility of the developed hydrogel formulations was evaluated using the MTT assay. Cells were exposed to hydrogel samples for

specified durations, followed by assessment of cell viability based on mitochondrial reduction of MTT reagent.

### 2.12 Stability Study

The optimized hydrogel formulation was subjected to stability studies under controlled storage conditions for three months. Physicochemical parameters including pH, viscosity, and drug content were periodically evaluated.

### 2.13 Statistical Analysis

All experiments were carried out in triplicate and results were expressed as mean  $\pm$  standard deviation. Statistical analysis was performed using Design-Expert® software and GraphPad Prism software. Analysis of variance (ANOVA) was used to determine statistical significance, with  $p < 0.05$  considered significant.

## 3. RESULTS AND DISCUSSION

### 3.1 Preformulation Studies

Preformulation studies were carried out to evaluate the physicochemical characteristics and compatibility of essential oils with selected excipients prior to formulation development.

#### 3.1.1 Organoleptic Evaluation

The essential oils exhibited characteristic appearance, odor, and clarity, confirming acceptable quality and purity.

**Table 1: Organoleptic Characteristics of Essential Oils**

Essential Oil	Color	Odor	Appearance
Eucalyptus oil	Pale yellow	Camphoraceous	Clear
Clove oil	Dark brown	Aromatic	Clear
Neem oil	Yellowish-brown	Characteristic pungent	Clear

#### 3.1.2 GC–MS Analysis

GC–MS analysis confirmed the presence of major bioactive compounds responsible for antimicrobial activity.



**Table 2: GC–MS Analysis of Essential Oils**

Essential Oil	Major Compound	Retention Time (min)	% Peak Area
Eucalyptus oil	1,8-Cineole	8.42	72.5
Clove oil	Eugenol	12.76	81.3
Neem oil	Azadirachtin	18.54	24.6

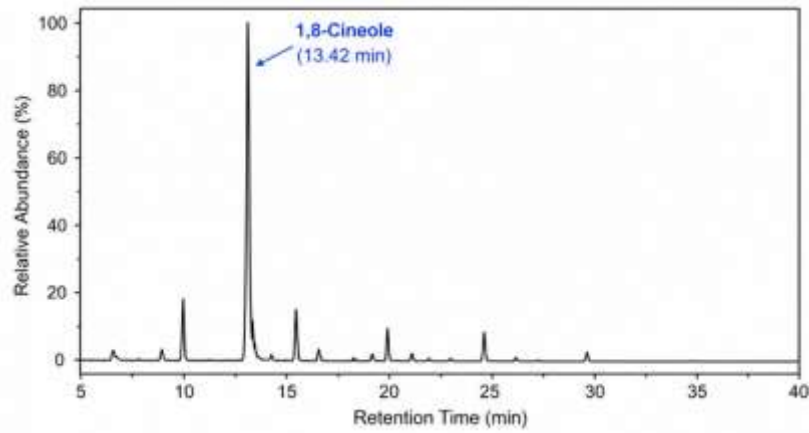


**Figure 1A: GC–MS Chromatogram of Eucalyptus Oil**

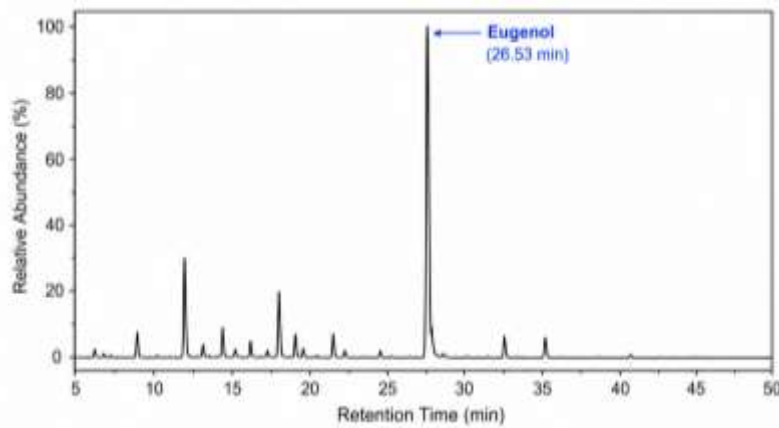


**Figure 1B: GC–MS Chromatogram of Clove Oil**

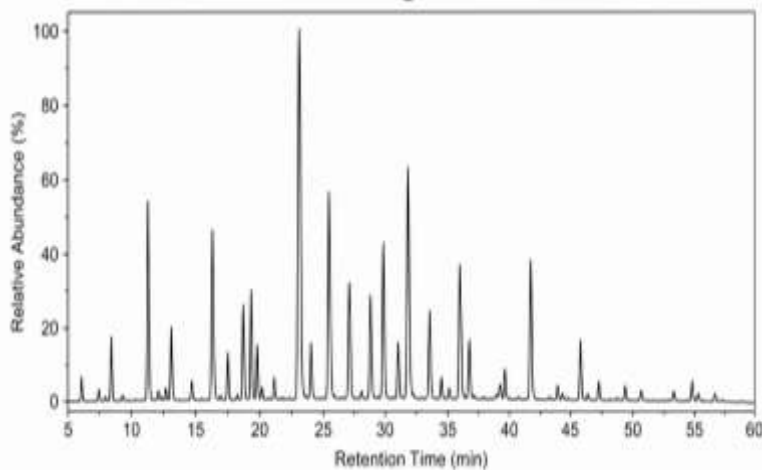


**Figure 1C: GC–MS Chromatogram of Neem Oil**

### 3.1.3 FT-IR Compatibility Study

FT-IR studies demonstrated retention of characteristic peaks corresponding to essential oils

and excipients, confirming absence of significant interaction.

**Table 3: FT-IR Peak Interpretation**

Component	Characteristic Peak (cm <sup>-1</sup> )	Functional Group
Eucalyptus oil	1050	C–O stretching
Clove oil	1510	Aromatic C=C
Carbomer	1700	C=O stretching
HPMC	3400	OH stretching

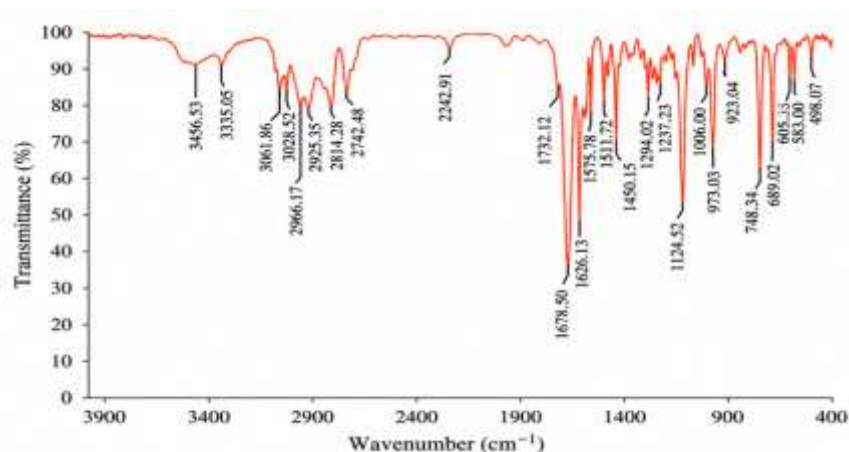


**Figure 2: FT-IR spectra showing compatibility between essential oils and selected excipients**

The GC–MS analysis confirmed the presence of 1,8-cineole and eugenol as major phytoconstituents, both of which are known for strong antimicrobial activity. FT-IR studies further confirmed compatibility between essential oils and formulation excipients, indicating suitability for hydrogel development.

### 3.2 Physicochemical Evaluation of Hydrogel Formulations

The prepared hydrogel formulations were evaluated for physicochemical parameters including pH, viscosity, spreadability, and drug content uniformity. These characteristics play a crucial role in determining the stability, applicability, patient acceptability, and overall therapeutic performance of topical hydrogel systems. The pH values of all formulations ranged

between  $5.58 \pm 0.02$  and  $5.67 \pm 0.01$ , indicating compatibility with normal skin pH. Maintaining formulation pH within the physiological skin range is essential to minimize irritation and ensure suitability for prolonged topical application. Viscosity values varied according to polymer concentration and surfactant content. Formulations containing higher polymer concentrations demonstrated increased viscosity due to enhanced polymer chain entanglement and formation of a denser gel matrix. The optimized formulation (F13) exhibited a viscosity of  $5200 \pm 150$  cP, which provided suitable consistency and retention at the site of application without compromising spreadability. Spreadability values demonstrated an inverse relationship with viscosity. Formulations with lower viscosity exhibited higher spreadability, facilitating easier

application over the infected tissue surface. The optimized formulation demonstrated balanced rheological behavior with a spreadability value of  $18.0 \pm 0.5$  g·cm/s. Drug content uniformity values

ranged from  $95.6 \pm 1.4\%$  to  $99.8 \pm 0.9\%$ , confirming homogeneous distribution of essential oils within the hydrogel matrix and effectiveness of the formulation process.

**Table 4: Physicochemical Evaluation of Hydrogel Formulations**

Batch	pH	Viscosity (cP)	Spreadability (g·cm/s)	Drug Content (%)
F1	$5.62 \pm 0.02$	$4820 \pm 120$	$18.5 \pm 0.6$	$96.2 \pm 1.3$
F2	$5.58 \pm 0.03$	$4950 \pm 140$	$17.8 \pm 0.5$	$97.5 \pm 1.2$
F3	$5.65 \pm 0.02$	$5100 \pm 150$	$19.2 \pm 0.7$	$98.1 \pm 1.1$
F4	$5.60 \pm 0.02$	$5250 \pm 160$	$18.6 \pm 0.6$	$99.3 \pm 1.0$
F5	$5.67 \pm 0.01$	$4300 \pm 110$	$21.5 \pm 0.8$	$95.6 \pm 1.4$
F6	$5.61 \pm 0.02$	$4400 \pm 120$	$20.8 \pm 0.7$	$97.0 \pm 1.3$
F7	$5.63 \pm 0.02$	$5600 \pm 180$	$16.5 \pm 0.5$	$98.8 \pm 1.2$
F8	$5.59 \pm 0.02$	$5750 \pm 190$	$15.9 \pm 0.4$	$99.6 \pm 1.1$
F9	$5.64 \pm 0.02$	$4500 \pm 130$	$20.5 \pm 0.7$	$97.9 \pm 1.2$
F10	$5.60 \pm 0.03$	$4650 \pm 140$	$19.8 \pm 0.6$	$98.5 \pm 1.1$
F11	$5.62 \pm 0.02$	$5850 \pm 200$	$15.2 \pm 0.4$	$99.1 \pm 1.0$
F12	$5.58 \pm 0.02$	$6000 \pm 210$	$14.8 \pm 0.3$	$99.8 \pm 0.9$
F13	$5.61 \pm 0.01$	$5200 \pm 150$	$18.0 \pm 0.5$	$98.9 \pm 1.0$

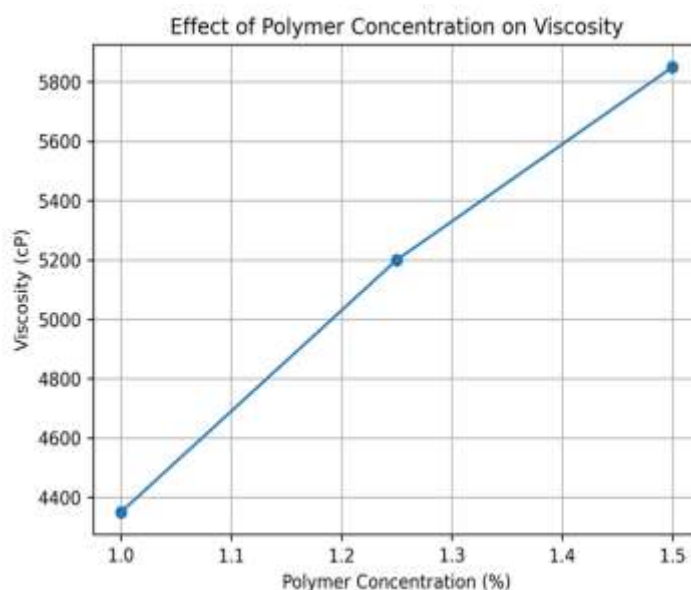


**Figure 3: Effect of polymer concentration on viscosity of hydrogel formulations.**

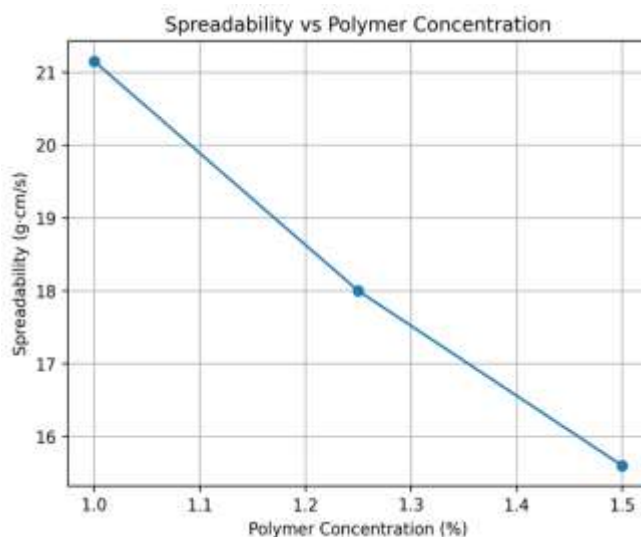


**Figure 4: Relationship between viscosity and spreadability of hydrogel formulations.**

The observed increase in viscosity with increasing polymer concentration can be attributed to stronger intermolecular interactions and enhanced structural rigidity within the hydrogel matrix. Similar rheological behaviour has been reported in previous studies involving carbomer-based hydrogels. The optimized formulation (F13) demonstrated balanced physicochemical properties, indicating suitability for topical administration and further biological evaluation.

### 3.3 In Vitro Drug Release Study

The in vitro drug release profiles of selected hydrogel formulations were evaluated over a period of 12 hours using Franz diffusion cells. All

formulations exhibited sustained release characteristics, confirming successful incorporation of essential oils within the hydrogel matrix. Formulation F5 demonstrated the highest cumulative drug release ( $96.5 \pm 3.0\%$ ) at 12 hours, followed by F9 and F13. Formulations containing higher polymer concentrations exhibited comparatively slower release profiles due to formation of a denser polymeric network that restricted diffusion of essential oil components. The optimized formulation (F13) exhibited cumulative drug release of  $93.1 \pm 2.7\%$  at 12 hours, indicating sustained and controlled release behaviour suitable for prolonged antimicrobial action at the site of infection.

**Table 5: In Vitro Drug Release Profile of Hydrogel Formulations**

Time (h)	F1	F5	F9	F13	F8
1	22.5 $\pm$ 1.2	28.3 $\pm$ 1.4	25.6 $\pm$ 1.3	24.8 $\pm$ 1.2	18.2 $\pm$ 1.1
4	48.2 $\pm$ 1.8	55.6 $\pm$ 2.0	52.1 $\pm$ 1.9	50.3 $\pm$ 1.7	42.5 $\pm$ 1.5
8	72.6 $\pm$ 2.3	80.1 $\pm$ 2.5	77.4 $\pm$ 2.4	75.2 $\pm$ 2.2	68.8 $\pm$ 2.1
12	91.2 $\pm$ 2.8	96.5 $\pm$ 3.0	94.3 $\pm$ 2.9	93.1 $\pm$ 2.7	89.5 $\pm$ 2.6

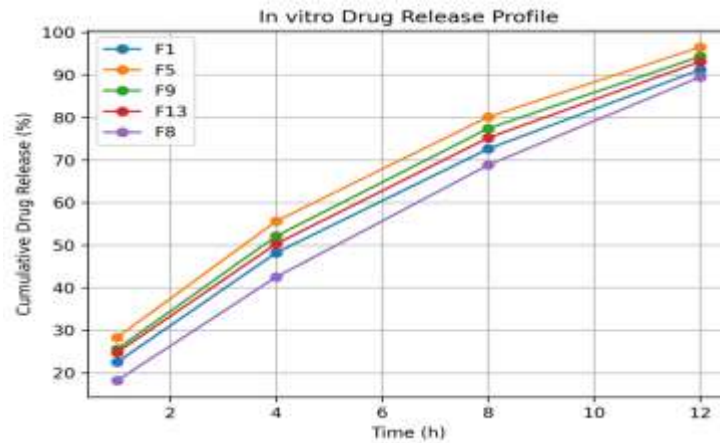


**Figure 5: In vitro drug release profile of selected hydrogel formulations.**

The sustained release pattern observed in the formulations is advantageous in topical antimicrobial therapy, as it ensures prolonged exposure of pathogens to active components while reducing frequency of application. The release behaviour was strongly influenced by polymer concentration and hydrogel viscosity. Formulations with moderate viscosity demonstrated balanced release and retention characteristics, contributing to improved therapeutic potential.

To understand the mechanism governing release of essential oil components from the hydrogel matrix, the release data were fitted into various kinetic models, including zero-order, first-order, Higuchi, and Korsmeyer–Peppas models. Among the tested models, the Korsmeyer–Peppas model exhibited the highest correlation coefficients ( $R^2$  values) for all selected formulations, indicating that release followed a non-Fickian diffusion mechanism involving both diffusion and polymer relaxation processes.

### 3.4 Drug Release Kinetics

**Table 6: Drug Release Kinetics Model Fitting ( $R^2$  Values)**

Formulation	Zero-order	First-order	Higuchi	Korsmeyer–Peppas
F1	0.942	0.981	0.968	0.992
F5	0.955	0.987	0.972	0.995
F9	0.948	0.984	0.970	0.993
F13	0.951	0.985	0.971	0.994
F8	0.938	0.979	0.965	0.991

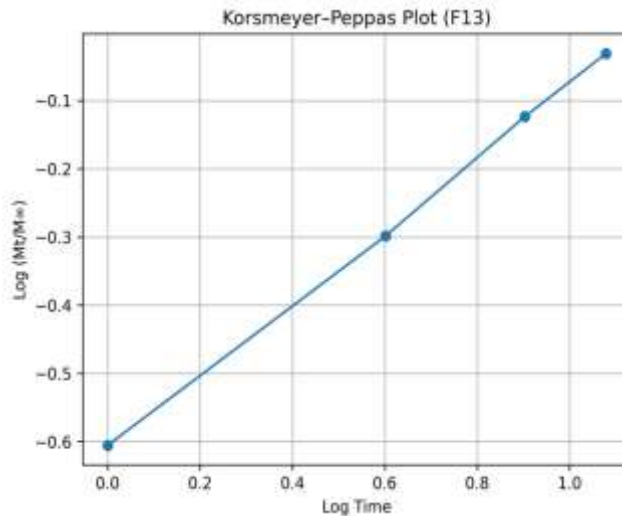


**Figure 6: Korsmeyer–Peppas model plot.**

The dominance of the Korsmeyer–Peppas model suggests that drug release occurred through a combined mechanism involving diffusion of active compounds through the hydrated matrix along with gradual relaxation and swelling of polymer chains. This type of release behaviour is considered beneficial for topical hydrogels intended for prolonged antimicrobial action, as it enables sustained delivery of essential oil components over an extended period.

### 3.5 Optimization and Statistical Analysis

The formulation variables were optimized using a Box–Behnken design. The experimental responses obtained were analyzed using analysis of variance (ANOVA) to determine the significance of independent variables on formulation performance. The statistical model was found to be highly significant ( $p < 0.0001$ ), indicating good agreement between predicted and observed responses.

**Table 7: ANOVA for Viscosity Response**

Source	Sum of Squares	df	Mean Square	F-value	p-value
Model	3.52E+06	9	3.91E+05	45.6	<0.0001
X <sub>1</sub>	1.12E+05	1	1.12E+05	13.1	0.006
X <sub>2</sub>	2.45E+05	1	2.45E+05	28.6	0.001
X <sub>3</sub>	2.80E+06	1	2.80E+06	326.5	<0.0001

**Table 8: Regression Statistics**

Parameter	Value
R <sup>2</sup>	0.987
Adjusted R <sup>2</sup>	0.975
Predicted R <sup>2</sup>	0.962
Adequate Precision	18.5

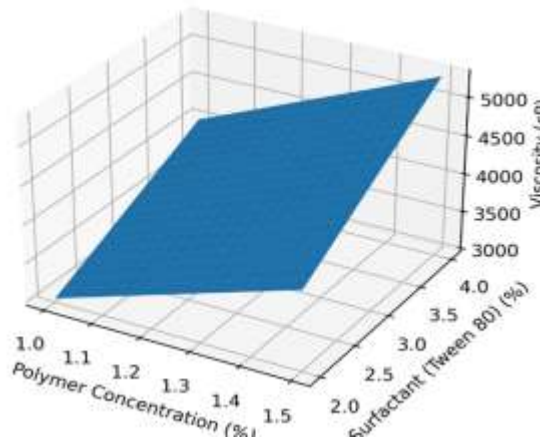


**Figure 7: Response surface plot showing effect of polymer and surfactant concentration on viscosity.**

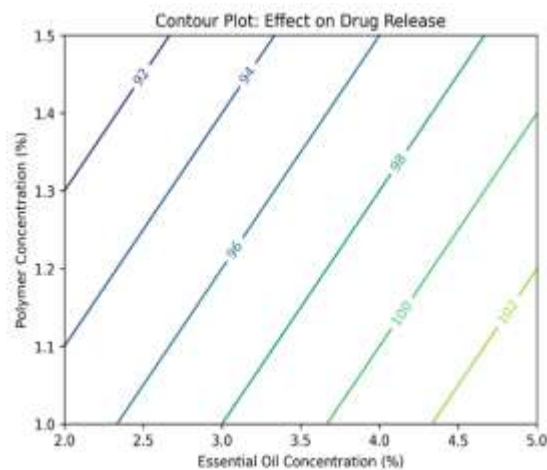


**Figure 8: Contour plot showing combined effect of essential oil concentration and polymer concentration on drug release.**

The high  $R^2$  value confirmed the suitability and predictive capability of the statistical model. Among the formulation variables, polymer concentration exerted the greatest influence on viscosity and drug release behavior. The optimized formulation (F13) was selected based on balanced physicochemical properties, sustained drug release, and predicted desirability criteria.

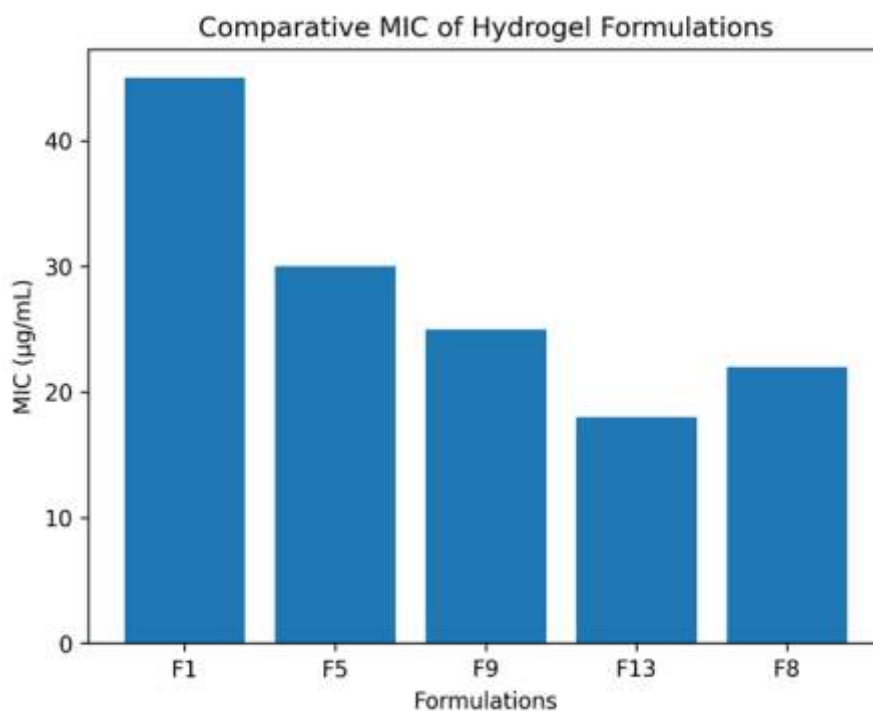
### 3.6 Antimicrobial Activity

The antimicrobial activity of the developed hydrogel formulations was evaluated against anaerobic pathogens associated with gas gangrene, including *Clostridium perfringens* and *Clostridium septicum*. The minimum inhibitory concentration (MIC) and minimum bactericidal

concentration (MBC) studies demonstrated significant antibacterial activity for all formulations, with formulation F13 exhibiting the highest efficacy. The MIC values ranged from 18  $\mu\text{g/mL}$  to 45  $\mu\text{g/mL}$ , while MBC values ranged from 36  $\mu\text{g/mL}$  to 90  $\mu\text{g/mL}$ . The optimized formulation (F13) demonstrated the lowest MIC and MBC values, indicating superior antimicrobial potency compared to other formulations. The enhanced activity observed in F13 may be attributed to the synergistic combination of eucalyptus, clove, and neem oils along with balanced polymeric composition that facilitated sustained release and improved diffusion of active constituents.

**Table 9: MIC and MBC Values of Hydrogel Formulations**

Formulation	MIC ( $\mu\text{g/mL}$ )	MBC ( $\mu\text{g/mL}$ )
F1	45	90
F5	30	60
F9	25	50
F13	18	36
F8	22	44

**Figure 9: Comparative MIC values of hydrogel formulations against anaerobic pathogens.**

The strong antimicrobial activity observed for F13 can primarily be attributed to the presence of eugenol and 1,8-cineole, which are known to disrupt bacterial cell membranes and interfere with intracellular metabolic processes. Neem oil further contributed supportive antimicrobial and anti-inflammatory effects. The results also indicated that formulations with moderate viscosity demonstrated improved antimicrobial activity compared to highly viscous systems, likely due to better release and diffusion of essential oil components.

### 3.7 Time–Kill Kinetics Study

Time–kill kinetics studies were performed to evaluate the bactericidal activity of the optimized formulation over time at concentrations corresponding to  $1\times$  MIC and  $2\times$  MIC. The formulation exhibited concentration-dependent bacterial killing, with complete eradication observed at  $2\times$  MIC within 24 hours. A significant reduction in viable bacterial count was also observed at  $1\times$  MIC.

**Table 10: Time–Kill Kinetics Data for Optimized Formulation (F13)**

Time (h)	Log CFU/mL ( $1\times$ MIC)	Log CFU/mL ( $2\times$ MIC)
0	$6.00 \pm 0.05$	$6.00 \pm 0.05$
2	$5.20 \pm 0.07$	$4.80 \pm 0.06$
4	$4.30 \pm 0.06$	$3.60 \pm 0.05$



8	3.10 ±0.05	2.00 ±0.04
12	2.20 ±0.04	1.20 ±0.03
24	1.10 ±0.03	0.00 ±0.00

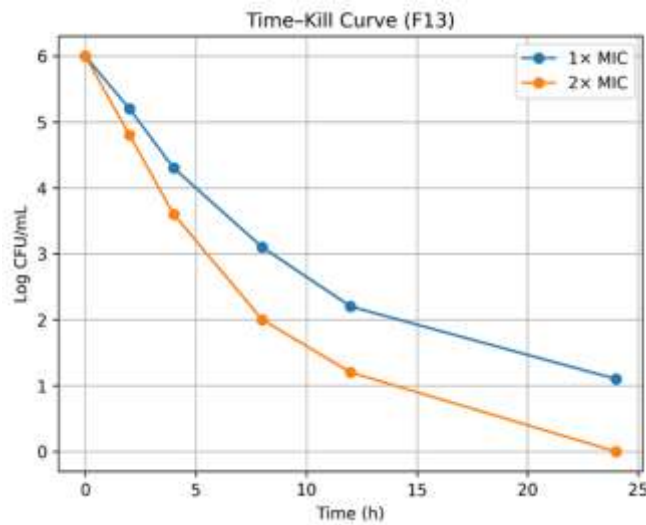


Figure 10: Time-kill kinetics curve of optimized hydrogel formulation.

The reduction greater than 3 log units within 24 hours confirmed the bactericidal nature of the optimized formulation. The rapid killing kinetics may be attributed to membrane disruption caused by essential oil constituents, leading to leakage of intracellular components and irreversible bacterial damage. The concentration-dependent behaviour observed in the study further supports the

suitability of the essential oil blend for treatment of severe anaerobic infections.

### 3.8 Synergistic Interaction of Essential Oils

The checkerboard assay demonstrated significant synergistic interactions among the selected essential oils. The triple combination exhibited the lowest FICI value (0.36), indicating strong synergistic interaction.

Table 11: FICI Values for Essential Oil Combinations

Combination	FICI Value	Interpretation
Eucalyptus + Clove	0.42	Synergistic
Clove + Neem	0.48	Synergistic
Eucalyptus + Neem	0.55	Additive
Triple Combination	0.36	Strong synergy

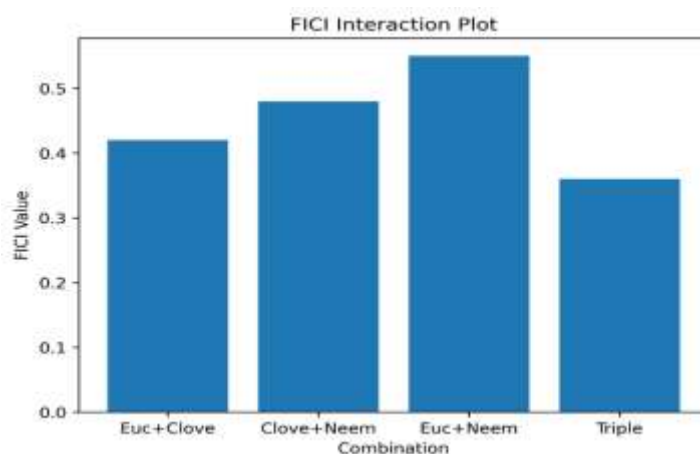


**Figure 11: FICI interaction plot showing synergistic effect among essential oil combinations.**

The synergistic interaction observed in the triple combination may be explained by complementary mechanisms of action. Eucalyptus oil enhanced membrane permeability, clove oil exerted potent bactericidal activity through eugenol, while neem oil contributed additional antimicrobial and wound-healing properties. The synergistic approach enabled enhanced antimicrobial efficacy at lower concentrations, thereby potentially reducing toxicity and irritation associated with higher concentrations of individual oils.

### 3.9 Antibiofilm Activity

The developed hydrogel formulations demonstrated significant antibiofilm activity against anaerobic pathogens. Formulation F13 exhibited the highest biofilm inhibition and eradication activity among all tested formulations. Biofilm inhibition values ranged from  $52.4 \pm 1.8\%$  to  $85.6 \pm 2.7\%$ , while biofilm eradication values ranged from  $45.6 \pm 1.6\%$  to  $80.2 \pm 2.6\%$ .

**Table 12: Biofilm Inhibition Activity of Hydrogel Formulations**

Formulation	Biofilm Inhibition (%)
F1	$52.4 \pm 1.8$
F5	$65.2 \pm 2.1$
F9	$72.8 \pm 2.4$
F13	$85.6 \pm 2.7$
F8	$78.3 \pm 2.5$

**Table 13: Biofilm Eradication Activity of Hydrogel Formulations**

Formulation	Biofilm Eradication (%)
F1	$45.6 \pm 1.6$
F5	$58.3 \pm 1.9$
F9	$66.5 \pm 2.2$
F13	$80.2 \pm 2.6$
F8	$72.4 \pm 2.3$

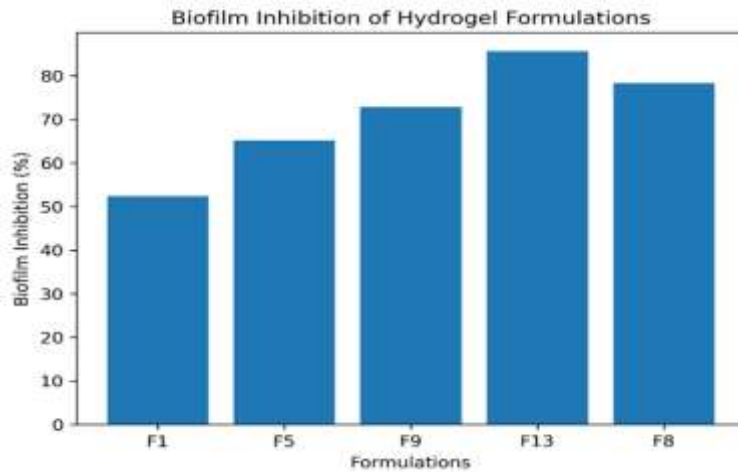


Figure 12: Biofilm inhibition activity of hydrogel formulations

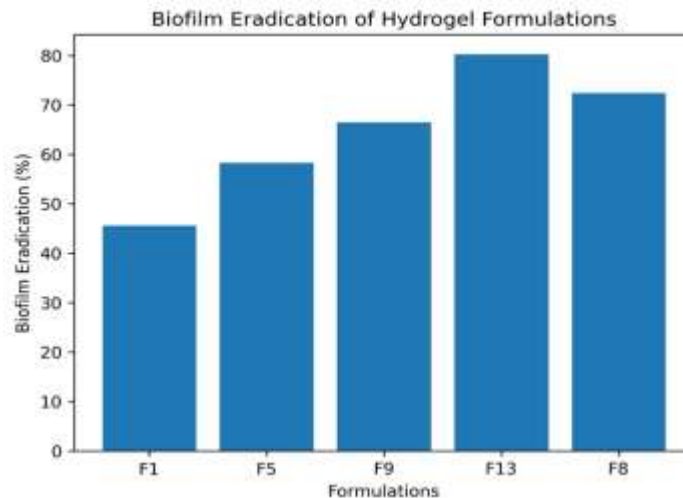


Figure 13: Biofilm eradication activity of hydrogel formulations.

The enhanced antibiofilm activity observed in the optimized formulation may be attributed to the ability of essential oil constituents to disrupt the extracellular polymeric matrix and interfere with quorum sensing pathways involved in biofilm formation. The lipophilic nature of essential oils facilitated penetration into the biofilm structure, resulting in destabilization and enhanced bacterial susceptibility.

### 3.10 Ex Vivo Permeation Study

Ex vivo permeation studies demonstrated enhanced permeation of essential oil components across biological membranes. The optimized formulation (F13) exhibited the highest flux and permeability coefficient among all tested formulations.

Table 14: Ex Vivo Permeation Parameters

Formulation	Flux ( $\mu\text{g}/\text{cm}^2/\text{hr}$ )	Permeability Coefficient (Kp)
F1	45.2 $\pm$ 1.5	0.045
F5	58.6 $\pm$ 1.8	0.058
F9	65.3 $\pm$ 2.0	0.065
F13	78.4 $\pm$ 2.4	0.078

F8	70.2 ±2.2	0.070
----	-----------	-------

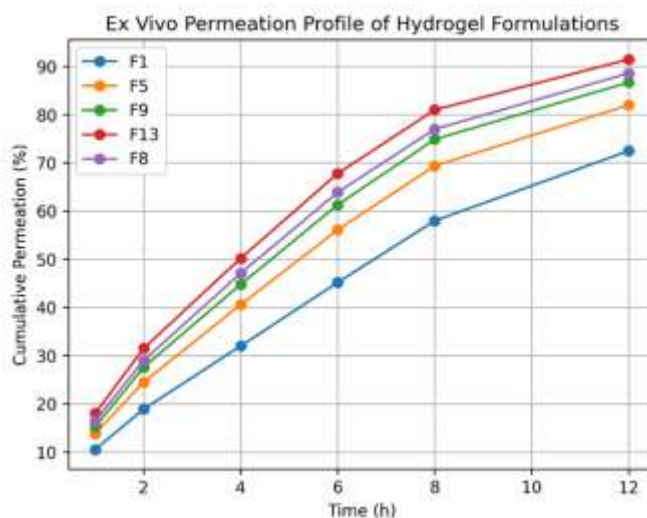


**Figure 14: Ex vivo permeation profile of selected hydrogel formulations.**

The enhanced permeation observed in F13 may be attributed to the presence of propylene glycol and eucalyptus oil, both of which are known penetration enhancers. The moderate viscosity of the optimized formulation also contributed to improved diffusion of active compounds across the membrane. Improved permeation is advantageous in topical therapy, as it facilitates

deeper penetration of antimicrobial agents into infected tissues and enhances therapeutic efficacy.

### 3.11 Cytocompatibility Study

The cytocompatibility of the developed hydrogel formulations was evaluated using the MTT assay. All formulations demonstrated acceptable cell viability values above 80%, indicating suitability for topical application.

**Table 15: Cell Viability of Hydrogel Formulations**

Formulation	Cell Viability (%)
F1	92.5 ±2.3
F5	90.8 ±2.1
F9	88.6 ±2.0
F13	86.4 ±1.9
F8	84.2 ±1.8

Although a slight decrease in cell viability was observed with increasing essential oil concentration, all formulations remained within acceptable biocompatibility limits. The optimized formulation exhibited satisfactory safety profile while maintaining strong antimicrobial activity.

### 3.12 Stability Studies

The optimized hydrogel formulation (F13) was subjected to stability studies for a period of three

months under controlled storage conditions to evaluate its physicochemical stability and retention of formulation characteristics over time. Parameters including pH, viscosity, and drug content were monitored periodically during the study period. The formulation exhibited minimal variation in all evaluated parameters, indicating acceptable stability and maintenance of formulation integrity throughout storage.

**Table 16: Stability Study Data of Optimized Formulation (F13)**

Parameter	Initial	1 Month	3 Months
pH	5.61	5.60	5.58
Viscosity (cP)	5200	5150	5100
Drug Content (%)	98.9	98.3	97.6

The slight reduction in viscosity observed during storage may be attributed to gradual relaxation of the polymeric network and minor changes in hydration behaviour of the hydrogel matrix. Similarly, the minimal reduction in drug content could be associated with limited volatilization or oxidation of essential oil constituents over time. However, the observed changes remained within acceptable pharmaceutical limits, confirming that the optimized formulation retained satisfactory stability under storage conditions. The stable pH profile further indicated that no significant chemical degradation or interaction occurred during the study period. These findings support the suitability of the developed hydrogel formulation for topical therapeutic application and potential long-term storage.

## CONCLUSION

The present study successfully developed and optimized a topical hydrogel formulation enriched with a synergistic blend of eucalyptus, clove, and neem essential oils for enhanced antimicrobial activity against anaerobic pathogens associated with gas gangrene. The hydrogel formulations exhibited acceptable physicochemical properties, including appropriate pH, viscosity, spreadability, and drug content uniformity. The optimized formulation (F13) demonstrated sustained drug release over 12 hours and followed Korsmeyer–Peppas release kinetics, indicating a non-Fickian diffusion mechanism. Significant antimicrobial activity was observed against anaerobic pathogens, with the optimized formulation exhibiting the lowest MIC and MBC values. Time–kill studies confirmed concentration-

dependent bactericidal activity, while checkerboard assays demonstrated strong synergistic interaction among the essential oils. The formulation also showed excellent antibiofilm activity, enhanced *ex vivo* permeation, acceptable cytocompatibility, and good stability over three months. The incorporation of essential oils into a hydrogel matrix effectively enhanced their stability, release behaviour, and antimicrobial efficacy. Overall, the findings indicate that the developed essential oil-enriched hydrogel represents a promising topical therapeutic system for the management of anaerobic wound infections and gas gangrene-associated complications.

## REFERENCES

- Adena, S. K. R., Herneisey, M., Pierce, E., Hartmeier, P. R., Adlakha, S., Hosfeld, M. A. I., Drennen, J. K., & Janjic, J. M. (2021). Quality by Design Methodology Applied to Process Optimization and Scale up of Curcumin Nanoemulsions Produced by Catastrophic Phase Inversion. *Pharmaceutics*, 13(6). <https://doi.org/10.3390/pharmaceutics13060880>
- Ahmed Khan, R., & van Vuuren, S. F. (2021). Essential oil combinations against *Clostridium perfringens* and *Clostridium septicum* - the causative agents of gas gangrene. *J Appl Microbiol*, 131(3), 1177-1192. <https://doi.org/10.1111/jam.15029>
- Alves, G. L., Teixeira, F. V., da Rocha, P. B. R., Krawczyk-Santos, A. P., Andrade, L. M., Cunha-Filho, M., Marreto, R. N., & Taveira, S. F. (2022). Preformulation and



- characterization of raloxifene-loaded lipid nanoparticles for transdermal administration. *Drug Deliv Transl Res*, 12(3), 526-537. <https://doi.org/10.1007/s13346-021-00949-y>
4. Ameer, A., Bensid, A., Ozogul, F., Ucar, Y., Durmus, M., Kulawik, P., & Boudjenah-Haroun, S. (2022). Application of oil-in-water nanoemulsions based on grape and cinnamon essential oils for shelf-life extension of chilled flathead mullet fillets. *J Sci Food Agric*, 102(1), 105-112. <https://doi.org/10.1002/jsfa.11336>
  5. Azevedo, S. G., Rocha, A. L. F., de Aguiar Nunes, R. Z., da Costa Pinto, C., Tălu, Ș., da Fonseca Filho, H. D., de Araújo Bezerra, J., Lima, A. R., Guimarães, F. E. G., Campelo, P. H., Bagnato, V. S., Inada, N. M., & Sanches, E. A. (2022). Pulsatile Controlled Release and Stability Evaluation of Polymeric Particles Containing Piper nigrum Essential Oil and Preservatives. *Materials (Basel)*, 15(15). <https://doi.org/10.3390/ma15155415>
  6. Azizpour, N., Partovi, R., Azizkhani, M., Abdulkhani, A., Babaei, A., Panahi, Z., & Samakkhah, S. A. (2025). Films of polylactic acid with graphene oxide-zinc oxide hybrid and Mentha longifolia essential oil: Effects on quality of refrigerated chicken fillet. *Int J Food Microbiol*, 426, 110893. <https://doi.org/10.1016/j.ijfoodmicro.2024.110893>
  7. Baccouri, O., Bendini, A., Cerretani, L., Guerfel, M., Baccouri, B., Lercker, G., Zarrouk, M., & Daoud Ben Miled, D. (2008). Comparative study on volatile compounds from Tunisian and Sicilian monovarietal virgin olive oils. *Food Chem*, 111(2), 322-328. <https://doi.org/10.1016/j.foodchem.2008.03.066>
  8. Beraldo-Araújo, V. L., Flávia Siqueira Vicente, A., van Vliet Lima, M., Umerska, A., Souto, E. B., Tajber, L., & Oliveira-Nascimento, L. (2022). Levofloxacin in nanostructured lipid carriers: Preformulation and critical process parameters for a highly incorporated formulation. *Int J Pharm*, 626, 122193. <https://doi.org/10.1016/j.ijpharm.2022.122193>
  9. Farruggia, D., Di Miceli, G., Licata, M., Leto, C., Salamone, F., & Novak, J. (2024). Foliar application of various biostimulants produces contrasting response on yield, essential oil and chemical properties of organically grown sage (*Salvia officinalis* L.). *Front Plant Sci*, 15, 1397489. <https://doi.org/10.3389/fpls.2024.1397489>
  10. Fernandes, L., Barco-Tejada, A., Blázquez, E., Araújo, D., Ribeiro, A., Silva, S., Cussó, L., Costa-de-Oliveira, S., Rodrigues, M. E., & Henriques, M. (2024). Development and Evaluation of Microencapsulated Oregano Essential Oil as an Alternative Treatment for *Candida albicans* Infections. *ACS Appl Mater Interfaces*, 16(31), 40628-40640. <https://doi.org/10.1021/acsami.4c07413>
  11. Filipe, G. A., Bigotto, B. G., Baldo, C., Gonçalves, M. C., Kobayashi, R. K. T., Lonni, A., & Celligoi, M. (2022). Development of a multifunctional and self-preserving cosmetic formulation using sophorolipids and palmarosa essential oil against acne-causing bacteria. *J Appl Microbiol*, 133(3), 1534-1542. <https://doi.org/10.1111/jam.15659>
  12. Fincheira, P., Espinoza, J., Levío-Raimán, M., Vera, J., Tortella, G., Brito, A. M. M., Seabra, A. B., Diez, M. C., Quiroz, A., & Rubilar, O. (2024). Formulation of essential oils-loaded solid lipid nanoparticles-based chitosan/PVA hydrogels to control the growth of *Botrytis cinerea* and *Penicillium expansum*. *Int J Biol Macromol*, 270(Pt 1), 132218.



- <https://doi.org/10.1016/j.ijbiomac.2024.132218>
13. Ghanouni, A., Avila, S. A., & Kim, H. J. (2022). Occult Colon Adenocarcinoma and Multiple Myeloma Associated With Clostridium septicum Panophthalmitis With Orbital and Chiasmal Extension: A Case Report. *Ophthalmic Plast Reconstr Surg*, 38(1), e6-e10. <https://doi.org/10.1097/iop.0000000000002056>
  14. Haimhoffer, Á., Dossi, E., Béresová, M., Bácskay, I., Váradi, J., Afsar, A., Rusznyák, Á., Vasvári, G., & Fenyvesi, F. (2021). Preformulation Studies and Bioavailability Enhancement of Curcumin with a 'Two in One' PEG- $\beta$ -Cyclodextrin Polymer. *Pharmaceutics*, 13(10). <https://doi.org/10.3390/pharmaceutics13101710>
  15. Huang, D., Li, H., Lin, Y., Lin, J., Li, C., Kuang, Y., Zhou, W., Huang, B., & Wang, P. (2022). Antibiotic-induced depletion of Clostridium species increases the risk of secondary fungal infections in preterm infants. *Front Cell Infect Microbiol*, 12, 981823. <https://doi.org/10.3389/fcimb.2022.981823>
  16. Ismail, T. A., Shehata, T. M., Mohamed, D. I., Elsewedy, H. S., & Soliman, W. E. (2021). Quality by Design for Development, Optimization and Characterization of Brucine Ethosomal Gel for Skin Cancer Delivery. *Molecules*, 26(11). <https://doi.org/10.3390/molecules26113454>
  17. Jain, P., Taleuzzaman, M., Kala, C., Kumar Gupta, D., Ali, A., & Aslam, M. (2021). Quality by design (Qbd) assisted development of phytosomal gel of aloe vera extract for topical delivery. *J Liposome Res*, 31(4), 381-388. <https://doi.org/10.1080/08982104.2020.1849279>
  18. Jia, Q., Xiang, H., Le, T., Wang, J., Chang, J., Wang, F., Sun, C., Tai, W., Jiang, Z., & Yin, X. (2025). A lipid nanoparticle encapsulated CPA-CTD mRNA vaccine provides protection against Clostridium perfringens-driven diseases. *Front Immunol*, 16, 1748171. <https://doi.org/10.3389/fimmu.2025.1748171>
  19. Koilpillai, J., & Narayanasamy, D. (2024). Development and characterization of novel surface engineered Depofoam: a QbD coupled failure modes and effects analysis risk assessment-based optimization studies. *J Liposome Res*, 34(1), 1-17. <https://doi.org/10.1080/08982104.2023.2208662>
  20. Qi, M., Hong, Y., Liu, Y., Wang, H., Xiong, Y., Tang, Y., Ma, M., Gao, Z., & Zhang, D. (2026). Carboxymethyl chitosan-based injectable hydrogel immobilizing single-atom nanozymes for localized ROS amplification and ferroptosis-enhanced postoperative oral cancer therapy. *Carbohydr Polym*, 373, 124668. <https://doi.org/10.1016/j.carbpol.2025.124668>
  21. Raj, A., Nirbhavane, P., Gandhi, H., Yadav, S., Kalra, A., & Sardana, S. (2026). Quality by design-driven approach to develop a nanocarrier-based sulfasalazine topical system for rheumatoid arthritis management. *Drug Dev Ind Pharm*, 1-13. <https://doi.org/10.1080/03639045.2026.2630260>
  22. Santonocito, D., Vivero-Lopez, M., Lauro, M. R., Torrisi, C., Castelli, F., Sarpietro, M. G., & Puglia, C. (2022). Design of Nanotechnological Carriers for Ocular Delivery of Mangiferin: Preformulation Study. *Molecules*, 27(4). <https://doi.org/10.3390/molecules27041328>



23. Sha, Z., Hao, M., Xue, X., Zhuo, F., Zhou, X., Lyu, T., Cui, Y., Gao, Y., Zhu, C., Jiang, B., Chen, Z., & Xu, L. (2026). Dual-enhanced transdermal delivery: Magnolol-borneol nanoparticle hydrogel for topical treatment of diabetic peripheral neuropathy. *Biomater Adv*, 182, 214676. <https://doi.org/10.1016/j.bioadv.2025.214676>
24. Sharma, M., Mazumder, R., & Debnath, A. (2026). Hydrogel-enabled drug delivery for ulcerative colitis. *Inflammopharmacology*. <https://doi.org/10.1007/s10787-026-02127-3>
25. Shi, H., Yang, K., Jiang, W., You, Y., Men, X., Wang, L., & Dang, C. (2026). Collision of hydrogels, chronic wounds, and nanotechnology: A bibliometric analysis from 2009 to 2024. *Colloids Surf B Biointerfaces*, 262, 115549. <https://doi.org/10.1016/j.colsurfb.2026.115549>
26. Singh, A. P., Kashaw, S. K., & Soni, V. (2026). Design, optimisation and in vivo evaluation of tazarotene loaded emulgel formulation for the treatment of acne. *J Drug Target*, 34(2), 215-223. <https://doi.org/10.1080/1061186x.2025.2546489>
27. Steele, G., & Austin, T. (2016). Preformulation investigations using small amounts of compound as an aid to candidate drug selection and early development. In *Pharmaceutical Preformulation and Formulation* (pp. 29-140). CRC Press.
28. Su, J., Liu, Z., Xiong, R., Zhu, R., Tong, Z., Liu, Y., & Xiao, R. (2026). A Two-Stage Cascading Amplification Strategy Based on Zn(2+)-Doped WO(X) Nanozymes for Ultrasensitive Lateral Flow Immunoassays of Clostridium Difficile Toxin B. *Adv Sci (Weinh)*, 13(3), e19130. <https://doi.org/10.1002/advs.202519130>
29. Tang, X., Qin, H., Zhang, X., Yang, H., Yang, J., Chen, P., Jin, Y., & Yang, L. (2024). Design, optimization, and evaluation for a long-time-released transdermal microneedle delivery system containing estradiol. *Drug Deliv Transl Res*, 14(6), 1551-1566. <https://doi.org/10.1007/s13346-023-01471-z>
30. Trinh, T. A., Phan, N. M., Nguyen, T. L., & Kim, J. (2026). Antioxidant Hydrogel-Based Transdermal Drug Delivery Patch for Reactive Oxygen Species- and MyD88-Targeted Management of Atopic Dermatitis. *Biomacromolecules*, 27(1), 121-133. <https://doi.org/10.1021/acs.biomac.5c00741>
31. Vater, C., Mannala, G. K., von Witzleben, M., Richter, R. F., Walter, N., Gelinsky, M., Alt, V., Lode, A., & Rupp, M. (2026). 3D Printing of Bacteriophage-Loaded Hydrogels: Development of a Local and Long-Lasting Delivery System. *Adv Healthc Mater*, 15(5), e03113. <https://doi.org/10.1002/adhm.202503113>
32. Vaz, R., Freitas, N., Sales, M. G. F., & Frasco, M. F. (2026). Photonic hydrogels for monitoring extracellular vesicle mimics. *Biosens Bioelectron*, 296, 118316. <https://doi.org/10.1016/j.bios.2025.118316>
33. Vemula, S. K., Narala, S., Uttreja, P., Narala, N., Daravath, B., Kalla, C. S. A., Baisa, S., Munnangi, S. R., Chella, N., & Repka, M. A. (2024). Quality by Design (QbD) Approach to Develop Colon-Specific Ketoprofen Hot-Melt Extruded Pellets: Impact of Eudragit(®) S 100 Coating on the In Vitro Drug Release. *Pharmaceutics*, 16(10). <https://doi.org/10.3390/pharmaceutics16101265>
34. Wang, A. J., Tian, H., Wang, Z. P., Cheng, J. X., Sun, J., Zhao, F., Shi, Y. J., Zhang, X. F., Zou, J. B., Luan, F., Zhai, B. T., & Guo, D. Y. (2026). An Injectable Photothermal Responsive Liposome Hydrogel Co-Loaded



- with Bufalin, Apatinib, and IR820 for Inhibiting Postoperative Recurrence of Colon Cancer. *Int J Nanomedicine*, 21, 575430. <https://doi.org/10.2147/ijn.S575430>
35. Weimer, P., Bordignon, I. M., Mineto, A. R., de Oliveira Araujo, K., Waszak, J. C., Brazil, N. T., Collares, F. M., Dul, M., Rossi, R. C., & Koester, L. S. (2026). Development of dissolving microneedles using a quality by design approach for transdermal delivery of the nanoemulsified volatile compound  $\beta$ -caryophyllene. *Int J Pharm*, 691, 126616. <https://doi.org/10.1016/j.ijpharm.2026.126616>
36. Woog, J. J., & Destro, M. (2022). Re: "Occult Colon Adenocarcinoma and Multiple Myeloma Associated With Clostridium septicum Panophthalmitis With Orbital and Chiasmal Extension: A Case Report". *Ophthalmic Plast Reconstr Surg*, 38(3), 306. <https://doi.org/10.1097/iop.0000000000002185>
37. Wu, Q., Yang, B., Wang, Y., Xiong, Y., Zhang, J., Wen, Y., & Rajkovic, A. (2025). A novel strategy for rapid, portable, and sensitive detection of Clostridium perfringens cpb2 gene using smartphone-based electrochemical DNA biosensor based on screen-printed electrodes modified with nanocomposite. *Mikrochim Acta*, 192(4), 264. <https://doi.org/10.1007/s00604-025-07126-9>
38. Xu, F., Xie, Y., Yu, W., & Wang, Z. (2026). Breaking the outer membrane barrier: structure, targets, and antimicrobial strategies for Gram-negative bacteria. *Front Microbiol*, 17, 1734749. <https://doi.org/10.3389/fmicb.2026.1734749>
39. Yang, J., Fang, X., Ma, Y., Xi, Z., Yang, W., & Feng, W. (2026). In vitro evaluation of antimicrobial activity of andrographolide against mixed biofilms of *Candida albicans* and *Staphylococcus aureus*. *BMC Complement Med Ther*. <https://doi.org/10.1186/s12906-026-05292-8>
40. Zhang, X., Zheng, H., Zhang, Y., Yang, X., Jin, N., Zhang, Q., & Chen, J. (2026). Design, fabrication, and evaluation of antimicrobial sponge-hydrogel bilayer microneedles: An integrated system for transdermal insulin delivery and glucose sensing. *Biomater Adv*, 182, 214693. <https://doi.org/10.1016/j.bioadv.2025.214693>

**HOW TO CITE:** Hritik, Dr. Puneet Kumar, Naresh Kumar, Development and Evaluation of Essential Oil-Enriched Topical Hydrogels for Antimicrobial Activity Against Anaerobic Pathogens Associated with Gas Gangrene, *Int. J. of Pharm. Sci.*, 2026, Vol 4, Issue 7, 1446-1467, <https://doi.org/10.5281/zenodo.21242405>

